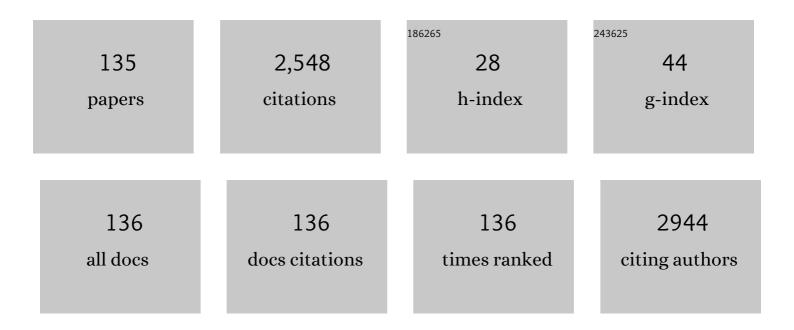
List of Publications by Year in descending order

Source: https://exaly.com/author-pdf/4077497/publications.pdf Version: 2024-02-01



#	Article	IF	CITATIONS
1	Optical absorption and light scattering in microcrystalline silicon thin films and solar cells. Journal of Applied Physics, 2000, 88, 148-160.	2.5	236
2	Organic–Inorganic Halide Perovskites: Perspectives for Silicon-Based Tandem Solar Cells. IEEE Journal of Photovoltaics, 2014, 4, 1545-1551.	2.5	123
3	Nanostructured three-dimensional thin film silicon solar cells with very high efficiency potential. Applied Physics Letters, 2011, 98, .	3.3	92
4	LYRA, a solar UV radiometer on Proba2. Advances in Space Research, 2006, 37, 303-312.	2.6	80
5	Formation of Continuous Nanocrystalline Diamond Layers on Glass and Silicon at Low Temperatures. Chemical Vapor Deposition, 2008, 14, 181-186.	1.3	77
6	Optical properties of SnO2:F films deposited by atmospheric pressure CVD. Thin Solid Films, 2009, 517, 6287-6289.	1.8	74
7	Optical properties of microcrystalline materials. Journal of Non-Crystalline Solids, 1998, 227-230, 967-972.	3.1	72
8	Silicon network relaxation in amorphous hydrogenated silicon. Physical Review B, 1997, 56, R12710-R12713.	3.2	68
9	Optical determination of the mass density of amorphous and microcrystalline silicon layers with different hydrogen contents. Journal of Non-Crystalline Solids, 1998, 227-230, 876-879.	3.1	65
10	Atmospheric pressure chemical vapour deposition of F doped SnO2 for optimum performance solar cells. Thin Solid Films, 2009, 517, 3061-3065.	1.8	58
11	Enhanced optical absorption in microcrystalline silicon. Journal of Non-Crystalline Solids, 1996, 198-200, 903-906.	3.1	52
12	Investigation of nanocrystalline diamond films grown on silicon and glass at substrate temperature below 400°C. Diamond and Related Materials, 2007, 16, 744-747.	3.9	51
13	Refractive indices of layers and optical simulations of Cu(In,Ga)Se ₂ solar cells. Science and Technology of Advanced Materials, 2018, 19, 396-410.	6.1	46
14	Growth of nanocrystalline diamond films deposited by microwave plasma CVD system at low substrate temperatures. Physica Status Solidi (A) Applications and Materials Science, 2006, 203, 3011-3015.	1.8	45
15	Amorphous silicon solar cells made with SnO2:F TCO films deposited by atmospheric pressure CVD. Materials Science and Engineering B: Solid-State Materials for Advanced Technology, 2009, 159-160, 6-9.	3.5	42
16	On the improvement of PEC activity of hematite thin films deposited by high-power pulsed magnetron sputtering method. Applied Catalysis B: Environmental, 2015, 165, 344-350.	20.2	41
17	Study of ZnO nanorods grown under UV irradiation. Applied Surface Science, 2019, 472, 105-111.	6.1	41
18	The optical absorption and photoconductivity spectra of hexagonal boron nitride single crystals. Physica Status Solidi A, 2005, 202, 2229-2233.	1.7	40

#	Article	IF	CITATIONS
19	Mechanism of photoconductivity in intrinsic epitaxial CVD diamond studied by photocurrent spectroscopy and photocurrent decay measurements. Diamond and Related Materials, 2005, 14, 556-560.	3.9	35
20	High-power pulsed plasma deposition of hematite photoanode for PEC water splitting. Catalysis Today, 2014, 230, 8-14.	4.4	32
21	Singleâ€Source, Solventâ€Free, Room Temperature Deposition of Black γ sSnI ₃ Films. Advanced Materials Interfaces, 2020, 7, 2000162.	3.7	32
22	Nanocrystalline diamond surface functionalization in radio frequency plasma. Diamond and Related Materials, 2006, 15, 745-748.	3.9	31
23	Performance of diamond detectors for VUV applications. Nuclear Instruments and Methods in Physics Research, Section A: Accelerators, Spectrometers, Detectors and Associated Equipment, 2006, 568, 398-405.	1.6	31
24	Chemical modifications and stability of diamond nanoparticles resolved by infrared spectroscopy and Kelvin force microscopy. Journal of Nanoparticle Research, 2013, 15, 1.	1.9	31
25	Deposition of hematite Fe2O3 thin film by DC pulsed magnetron and DC pulsed hollow cathode sputtering system. Thin Solid Films, 2013, 549, 184-191.	1.8	31
26	Enhancing the optoelectronic properties of amorphous zinc tin oxide by subgap defect passivation: A theoretical and experimental demonstration. Physical Review B, 2017, 95, .	3.2	31
27	Time of flight study of high performance CVD diamond detector devices. Physica Status Solidi (A) Applications and Materials Science, 2007, 204, 3023-3029.	1.8	29
28	Properties of boron-doped epitaxial diamond layers grown on (110) oriented single crystal substrates. Diamond and Related Materials, 2015, 53, 29-34.	3.9	29
29	Synthesis of zinc oxide nanostructures and comparison of their crystal quality. Applied Surface Science, 2018, 461, 190-195.	6.1	29
30	Double hollow cathode plasma jet-low temperature method for the TiO2â^'N photoresponding films. Electrochimica Acta, 2010, 55, 1548-1556.	5.2	26
31	Precursor gas composition optimisation for large area boron doped nano-crystalline diamond growth by MW-LA-PECVD. Carbon, 2018, 128, 164-171.	10.3	26
32	Spectral response of amorphous–nano-crystalline silicon thin films. Journal of Non-Crystalline Solids, 2008, 354, 2286-2290.	3.1	24
33	Preparation and optical properties of nanocrystalline diamond coatings for infrared planar waveguides. Thin Solid Films, 2016, 618, 130-133.	1.8	23
34	Design and investigation of properties of nanocrystalline diamond optical planar waveguides. Optics Express, 2013, 21, 8417.	3.4	22
35	Study of the surface properties of ZnO nanocolumns used for thin-film solar cells. Beilstein Journal of Nanotechnology, 2017, 8, 446-451.	2.8	22
36	The RF plasma surface chemical modification of nanodiamond films grown on glass and silicon at low temperature. Diamond and Related Materials, 2007, 16, 671-674.	3.9	21

#	Article	IF	CITATIONS
37	Structural, optical and mechanical properties of thin diamond and silicon carbide layers grown by low pressure microwave linear antenna plasma enhanced chemical vapour deposition. Diamond and Related Materials, 2016, 69, 13-18.	3.9	20
38	Growth Inhibition of Gram-Positive and Gram-Negative Bacteria by Zinc Oxide Hedgehog Particles. International Journal of Nanomedicine, 2021, Volume 16, 3541-3554.	6.7	20
39	Comparison of photocurrent spectra measured by FTPS and CPM for amorphous silicon layers and solar cells. Journal of Non-Crystalline Solids, 2008, 354, 2167-2170.	3.1	18
40	Optical study of defects in nanoâ€diamond films grown in linear antenna microwave plasma CVD from H ₂ /CH ₄ /CO ₂ gas mixture. Physica Status Solidi (B): Basic Research, 2012, 249, 2635-2639.	1.5	18
41	Arrays of ZnO nanocolumns for 3-dimensional very thin amorphous and microcrystalline silicon solar cells. Thin Solid Films, 2013, 543, 110-113.	1.8	18
42	Erbium ion implantation into diamond – measurement and modelling of the crystal structure. Physical Chemistry Chemical Physics, 2017, 19, 6233-6245.	2.8	18
43	Photocurrent Spectroscopy of Perovskite Layers and Solar Cells: A Sensitive Probe of Material Degradation. Journal of Physical Chemistry Letters, 2017, 8, 838-843.	4.6	18
44	Optically transparent composite diamond/Ti electrodes. Carbon, 2017, 119, 179-189.	10.3	18
45	High optical quality nanocrystalline diamond with reduced non-diamond contamination. Diamond and Related Materials, 2010, 19, 453-456.	3.9	17
46	ZnO hedgehog-like structures for control cell cultivation. Applied Surface Science, 2012, 258, 3485-3489.	6.1	17
47	Diamond-coated ATR prism for infrared absorption spectroscopy of surface-modified diamond nanoparticles. Applied Surface Science, 2013, 270, 411-417.	6.1	17
48	Exciton diffusion length in some thermocleavable polythiophenes by the surface photovoltage method. Synthetic Metals, 2012, 161, 2727-2731.	3.9	15
49	Effect of plasma composition on nanocrystalline diamond layers deposited by a microwave linear antenna plasmaâ€enhanced chemical vapour deposition system. Physica Status Solidi (A) Applications and Materials Science, 2015, 212, 2418-2423.	1.8	15
50	The infrared optical absorption spectra of the functionalized nanocrystalline diamond surface. Diamond and Related Materials, 2009, 18, 772-775.	3.9	14
51	The Optical Spectra of a-Si:H and a-SiC:H Thin Films Measured by the Absolute Photothermal Deflection Spectroscopy (PDS). Solid State Phenomena, 0, 213, 19-28.	0.3	14
52	Temperature dependence of intrinsic infrared absorption in natural and chemical-vapor deposited diamond. Journal of Applied Physics, 2002, 92, 756-763.	2.5	13
53	Amplitude modulated step scan Fourier transform photocurrent spectroscopy of partly compensated Bâ€doped CVD diamond thin films. Physica Status Solidi (A) Applications and Materials Science, 2007, 204, 2950-2956.	1.8	13
54	Control of tin oxide film morphology by addition of hydrocarbons to the chemical vapour deposition process. Thin Solid Films, 2010, 519, 1334-1340.	1.8	13

#	Article	IF	CITATIONS
55	Grazing angle reflectance spectroscopy of organic monolayers on nanocrystalline diamond films. Diamond and Related Materials, 2011, 20, 882-885.	3.9	13
56	Epoxy catalyzed sol–gel method for pinhole-free pyrite FeS2 thin films. Journal of Alloys and Compounds, 2014, 607, 169-176.	5.5	13
57	Structural, optical and electrical properties of nanodiamond films deposited by HFCVD on borosilicate glass, fused silica and silicon at low temperature. Physica Status Solidi A, 2004, 201, 2499-2502.	1.7	12
58	Substrate temperature changes during molecular beam epitaxy growth of GaMnAs. Journal of Applied Physics, 2007, 102, .	2.5	12
59	Deposition of nanocrystalline diamond films on temperature sensitive substrates for infrared reflectance spectroscopy. Physica Status Solidi (B): Basic Research, 2011, 248, 2736-2739.	1.5	12
60	Exciton diffusion length and concentration of holes in MEH-PPV polymer using the surface voltage and surface photovoltage methods. Chemical Physics Letters, 2012, 552, 49-52.	2.6	12
61	Thermal sulfidation of α-Fe2O3 hematite to FeS2 pyrite thin electrodes: Correlation between surface morphology and photoelectrochemical functionality. Catalysis Today, 2018, 313, 224-230.	4.4	12
62	Nanostructured Diamond Layers Enhance the Infrared Spectroscopy of Biomolecules. Langmuir, 2014, 30, 2054-2060.	3.5	11
63	Ferromagnetism appears in nitrogen implanted nanocrystalline diamond films. Journal of Magnetism and Magnetic Materials, 2015, 394, 477-480.	2.3	11
64	Raman scattering in boron doped nanocrystalline diamond films: Manifestation of Fano interference and phonon confinement effect. Solid State Communications, 2018, 276, 33-36.	1.9	11
65	Optical characterization of low temperature amorphous MoOx, WOX, and VOx prepared by pulsed laser deposition. Thin Solid Films, 2020, 693, 137690.	1.8	11
66	Hydrothermally grown ZnO:Mo nanorods exposed to X-ray: Luminescence and charge trapping phenomena. Applied Surface Science, 2022, 585, 152682.	6.1	11
67	Technological possibilities of Si:H thin film deposition with embedded cubic Mg ₂ Si nanoparticles. Physica Status Solidi C: Current Topics in Solid State Physics, 2013, 10, 1712-1716.	0.8	10
68	Optical properties of p–i–n structures based on amorphous hydrogenated silicon with silicon nanocrystals formed via nanosecond laser annealing. Semiconductors, 2016, 50, 935-940.	0.5	10
69	Nanodiamond surface chemistry controls assembly of polypyrrole and generation of photovoltage. Scientific Reports, 2021, 11, 590.	3.3	10
70	Enhanced Photodegradation in Metal Oxide Nanowires with Co-Doped Surfaces under a Low Magnetic Field. ACS Applied Materials & Interfaces, 2021, 13, 23173-23180.	8.0	10
71	Solar-Blind Diamond Detectors for Lyra, the Solar VUV Radiometer on Board Proba II. Experimental Astronomy, 2003, 16, 141-148.	3.7	9
72	On the reduction of the non-diamond phase in nanocrystalline CVD diamond films. Diamond and Related Materials, 2009, 18, 726-729.	3.9	9

#	Article	IF	CITATIONS
73	Optimum performance solar cells using atmospheric pressure chemical vapour deposition deposited TCOs. International Journal of Nanotechnology, 2009, 6, 816.	0.2	9
74	Fourier transform photocurrent measurement of thin silicon films on rough, conductive and opaque substrates. Physica Status Solidi (A) Applications and Materials Science, 2010, 207, 578-581.	1.8	9
75	Optical characterisation of organosilane-modified nanocrystalline diamond films. Chemical Papers, 2011, 65, .	2.2	9
76	Nâ€Vâ€related fluorescence of the monoenergetic highâ€energy electronâ€irradiated diamond nanoparticles. Physica Status Solidi (A) Applications and Materials Science, 2015, 212, 2519-2524.	1.8	9
77	Synthesis and properties of diamond - silicon carbide composite layers. Journal of Alloys and Compounds, 2019, 800, 327-333.	5.5	9
78	Local Variations and Temperature Dependence of Optical Absorption Coefficient in Natural IIa Type and CVD Diamond Optical Windows. Physica Status Solidi A, 2001, 186, 297-301.	1.7	8
79	Photocurrent study of electronic defects in nanocrystalline diamond. Diamond and Related Materials, 2008, 17, 1311-1315.	3.9	8
80	Towards opticalâ€quality nanocrystalline diamond with reduced nonâ€diamond content. Physica Status Solidi (A) Applications and Materials Science, 2009, 206, 2004-2008.	1.8	8
81	The optical absorption of metal nanoparticles deposited on ZnO films. Physica Status Solidi (A) Applications and Materials Science, 2010, 207, 1722-1725.	1.8	8
82	Electrical and optical characteristics of boron doped nanocrystalline diamond films. Vacuum, 2019, 168, 108813.	3.5	8
83	Room temperature plasma hydrogenation – An effective way to suppress defects in ZnO nanorods. Materials Today: Proceedings, 2020, 33, 2481-2483.	1.8	8
84	Photo-Hall effect measurements in P, N and B-doped diamond at low temperatures. Diamond and Related Materials, 2004, 13, 713-717.	3.9	7
85	Coâ€implantation of Er and Yb ions into singleâ€crystalline and nanoâ€crystalline diamond. Surface and Interface Analysis, 2018, 50, 1218-1223.	1.8	7
86	Charge trapping processes in hydrothermally grown Er-doped ZnO. Radiation Measurements, 2022, 150, 106700.	1.4	7
87	Free-Standing ZnO:Mo Nanorods Exposed to Hydrogen or Oxygen Plasma: Influence on the Intrinsic and Extrinsic Defect States. Materials, 2022, 15, 2261.	2.9	7
88	Why Does Diamond Absorb Infra-Red Radiation?. Physica Status Solidi A, 2002, 193, 442-447.	1.7	6
89	Spectroscopy of thin nanodiamond layers and membranes. Journal of Non-Crystalline Solids, 2006, 352, 1344-1347.	3.1	6
90	Siâ€related color centers in nanocrystalline diamond thin films. Physica Status Solidi (B): Basic Research, 2014, 251, 2603-2606.	1.5	6

#	Article	IF	CITATIONS
91	Formation and study of p–i–n structures based on two-phase hydrogenated silicon with a germanium layer in the i-type region. Semiconductors, 2017, 51, 1370-1376.	0.5	6
92	Optical properties of the plasma hydrogenated ZnO thin films. Journal of Electrical Engineering, 2017, 68, 70-73.	0.7	6
93	Scanning Tunneling Microscopy and Spectroscopy of Non-Doped, Hydrogen Terminated CVD Diamond. Physica Status Solidi A, 2000, 181, 77-81.	1.7	5
94	Defect-dopant interaction in n- and p-type diamond and its influence on electrical properties. Diamond and Related Materials, 2004, 13, 722-726.	3.9	5
95	Erbium Luminescence Centres in Single- and Nano-Crystalline Diamond—Effects of Ion Implantation Fluence and Thermal Annealing. Micromachines, 2018, 9, 316.	2.9	5
96	Optoelectronic Properties of Hydrogenated Amorphous Substoichiometric Silicon Carbide with Low Carbon Content Deposited on Semiâ€Transparent Boronâ€Doped Diamond. Physica Status Solidi (A) Applications and Materials Science, 2019, 216, 1900241.	1.8	5
97	Maximized vertical photoluminescence from optical material with losses employing resonant excitation and extraction of photonic crystal modes. Nanophotonics, 2019, 8, 1041-1050.	6.0	5
98	Electroluminescence of thin film <i>p-i-n</i> diodes based on a-SiC:H with integrated Ge nanoparticles. EPJ Applied Physics, 2019, 88, 30302.	0.7	5
99	Photo-Hall measurements on phosphorus-doped n-type CVD diamond at low temperatures. Physica Status Solidi A, 2003, 199, 82-86.	1.7	4
100	The influence of thermal annealing on the electronic defect states in nanocrystalline CVD diamond films. Physica Status Solidi (A) Applications and Materials Science, 2008, 205, 2158-2162.	1.8	4
101	Optimization of Solar Cell Performance using Atmospheric Pressure Chemical Vapour Deposition deposited TCOs. ECS Transactions, 2009, 25, 789-796.	0.5	4
102	INFRARED PHOTOLUMINESCENCE SPECTRA OF PBS NANOPARTICLES PREPARED BY LANGMUIR–BLODGETT AND LASER ABLATION METHODS. Acta Polytechnica, 2014, 54, 426-429.	0.6	4
103	Nickel oxide films by thermal annealing of ion-beam-sputtered Ni: Structure and electro-optical properties. Thin Solid Films, 2017, 640, 52-59.	1.8	4
104	Highâ€Temperature PIN Diodes Based on Amorphous Hydrogenated Siliconâ€Carbon Alloys and Boronâ€Doped Diamond Thin Films. Physica Status Solidi (B): Basic Research, 2020, 257, 1900247.	1.5	4
105	Pulsed laser deposition of high-transparency molybdenum oxide thin films. Vacuum, 2021, 194, 110613.	3.5	4
106	Microscopic Study of Bovine Serum Albumin Adsorption on Zinc Oxide (0001) Surface. Physica Status Solidi (A) Applications and Materials Science, 2021, 218, 2000558.	1.8	4
107	Surface and Ultrathin-layer Absorptance Spectroscopy for Solar Cells. Energy Procedia, 2014, 60, 57-62.	1.8	3
108	Fabrication of diamond-coated germanium ATR prisms for IR-spectroscopy. Vibrational Spectroscopy, 2016, 84, 67-73.	2.2	3

#	Article	IF	CITATIONS
109	Manipulation of the magnetoabsorption effect in Co-coated ZnO nanowires with Au decoration. Applied Surface Science, 2019, 492, 591-597.	6.1	3
110	Photothermal Deflection Mapping of Variations in the Optical Absorption in IR Windows. Physica Status Solidi A, 2000, 181, 115-119.	1.7	2
111	Infrared optical properties of heavily B-doped nanocrystalline diamond films on low alkaline glass substrates. Physica Status Solidi (A) Applications and Materials Science, 2006, 203, 3016-3020.	1.8	2
112	Study of the passivation mechanisms of boron doped diamond using the Amplitude Modulated Step Scan Fourier Transform Photocurrent Spectroscopy. Diamond and Related Materials, 2009, 18, 827-830.	3.9	2
113	Laser profiling of defects in BaWO4crystals. Measurement Science and Technology, 2012, 23, 087001.	2.6	2
114	Multiple kinds of emission modes in semiconductor microcavity coupled with plasmon. Physica B: Condensed Matter, 2014, 434, 74-77.	2.7	2
115	plasma HYDROGENATION OF HYDROTHERMALLY GROWN ZnO MICROPODS. , 2020, , .		2
116	Deposition of magnesium silicide nanoparticles by the combination of vacuum evaporation and hydrogen plasma treatment. , 0, , .		2
117	Transformation of ZnO-based structures under heavy Mo doping: defect states and luminescence. , 2021, , .		2
118	Single Crystal CVD Diamond growth and characterizations. Materials Research Society Symposia Proceedings, 2006, 956, 1.	0.1	1
119	Optical absorption losses in metal layers used in thin film solar cells. Physica Status Solidi (A) Applications and Materials Science, 2010, 207, 2170-2173.	1.8	1
120	Photoluminescence eigenmodes in the ZnO semiconductor microcavity on the Ag/Si substrate. Applied Physics A: Materials Science and Processing, 2013, 112, 821-825.	2.3	1
121	Manipulated Optical Absorption and Accompanied Photocurrent Using Magnetic Field in Charger Transfer Engineered C/ZnO Nanowires. Global Challenges, 2020, 4, 2000025.	3.6	1
122	Single-Source Pulsed Laser Deposition of MAPbI3. , 2021, , .		1
123	Changes of morphological, optical and electrical properties induced by hydrogen plasma on (0001) ZnO Surface. Physica Status Solidi (A) Applications and Materials Science, 0, , 2100427.	1.8	1
124	Plasma Treatment of Gaâ€Doped ZnO Nanorods. Physica Status Solidi (A) Applications and Materials Science, 2022, 219, .	1.8	1
125	Comparison Between Chemical and Plasmatic Treatment of Seeding Layer for Patterned Diamond Growth. Materials Research Society Symposia Proceedings, 2009, 1203, 1.	0.1	0
126	Optical Monitoring of Nanocrystalline Diamond with Reduced Non-diamond Contamination. Materials Research Society Symposia Proceedings, 2009, 1203, 1.	0.1	0

#	Article	IF	CITATIONS
127	BaWO <inf>4</inf> intracavity pumped eye-safe Raman laser. , 2014, , .		0
128	Production of zinc oxide nanowires power with precisely defined morphology. Journal of Electrical Engineering, 2017, 68, 66-69.	0.7	0
129	Measurement of doping profiles by a contactless method of IR reflectance under grazing incidence. Review of Scientific Instruments, 2018, 89, 063114.	1.3	0
130	Ytterbium silicide nanostructures prepared by pulsed laser ablation in oven: Structural and electrical characterization. Materials Letters, 2019, 246, 17-19.	2.6	0
131	Effect of a-Si on CH3NH3PbI3 Films and Applications in Perovskite Solar Cells. , 2019, , .		0
132	Microscopic Study of Bovine Serum Albumin Adsorption on Zinc Oxide (0001) Surface. Physica Status Solidi (A) Applications and Materials Science, 2021, 218, 2170024.	1.8	0
133	Nanocrystalline diamond films heavily doped by boron: structure, optical and electrical properties. , 2019, , .		0
134	Emergence of DARK ZnO Nanorods by Hydrogen Plasma Treatment. , 2021, , .		0
135	Plasma-synthesised Zinc oxide nanoparticle behavior in liquids. , 2021, , .		0